IET Optoelectronics

Special Issue: Selected Papers from the 29th Semiconductor and Integrated OptoElectronics (SIOE) 2015

Mechanism for enhanced wavelength tuning in gain-levered InP quantum dot lasers

ISSN 1751-8768
Received on 12th June 2015
Revised on 25th August 2015
Accepted on 15th September 2015
doi: 10.1049/iet-opt.2015.0062
www.ietdl.org

Robert Thomas[1] ✉, *Daniel Briglin*[1], *Andrey B. Krysa*[2], *Peter Michael Smowton*[1]

[1]*School of Physics and Astronomy, Cardiff University, The Parade, Cardiff CF24 3AA, UK*
[2]*EPSRC National Centre for III-V Technologies, University of Sheffield, Sheffield, UK*
✉ *E-mail: thomasr25@cardiff.ac.uk*

Abstract: Peak gain wavelength tuning via the gain-lever effect is demonstrated in segmented contact InP quantum dot Fabry–Perot lasers. A tuning range of 6.5 ± 0.1 nm was recorded in the lasing spectra of a 1.9 mm long broad area device operating at 22°C. The authors clarify the nature of the tuning mechanism and identify the critical material and device parameters that determine the limits of the wavelength tuning range.

1 Introduction

Wavelength tunable semiconductor lasers are important for applications in telecoms [1, 2] and optical sensing [3–5]. Recently, the emergence of new fluorochromes for biosensing applications and the desire for improved excitation of old ones have led to an increasing demand for visible wavelength tunable lasers [6]. As with telecoms and gas sensing applications, large tuning ranges and fast tuning rates are desirable but linewidth constraints are somewhat relaxed due to the broad excitation bandwidth of the fluorochromes. Furthermore, when considering the miniaturisation of biosensor technologies to chip-based platforms, fabrication and operational simplicity becomes essential.

There are three main approaches to wavelength tuning with semiconductor lasers: external cavity lasers (ECLs) [7], distributed feedback (DFB) arrays [8] and sampled-grating distributed Bragg reflector (SG-DBR) devices [9]. While the tuning ranges that can be achieved using these approaches are comparable, typically tens of nanometres, ECLs and DFB devices, where the tuning control mechanisms are the movement of a mirror and the temperature control of the refractive index, respectively, have tuning rates that are slow (∼ ms). SG-DBR devices, on the other hand, can have fast tuning rates (of the order of nanoseconds) but precise control of as many as five separate inputs is required to isolate the desired wavelength making them more complex to manufacture and operate. In each of these approaches, a mode selection filter generated by optical feedback is tuned across the material gain spectrum to select a single axial mode of the laser cavity. Provided there is sufficient optical gain at the wavelength of the selected mode, the device will lase. The wavelength of the laser, therefore, is not determined by the peak of the gain spectrum as it is in a simple Fabry–Perot (FP) laser, but by the peak of the optical feedback spectrum.

Wavelength tuning is possible in FP lasers using the gain-lever effect to vary the optical path length of the laser cavity [10]. However, the tuning range available with this mechanism is limited to one axial mode spacing. In this work, we demonstrate how large-scale wavelength tuning can be achieved in FP lasers using the gain-lever effect to tune the wavelength peak of an InP quantum dot active material. This tuning is both rapid (sub-μs) and can be implemented in a simple structure that is easily fabricated, ideal for chip-based bio-sensing applications. Gain-levered quantum dot lasers can also offer enhanced modulation bandwidth [11]. We determine the limits of the tuning range and describe how device design can be optimised to generate the maximum tuning range for a given material.

2 Gain-lever effect

2.1 Wavelength tuning

A consequence of the sub-linear gain-carrier density relations found in semiconductor lasers is that a differential current injection along the length of a laser cavity, via a segmented electrical contact [10], provides a mechanism for controlling the above threshold average carrier density of the laser cavity: the gain-lever effect [12]. Fig. 1 is a schematic diagram of 50 μm oxide isolated stripe segmented contact cleaved facet lasers used in this work. The segmented contacts are electrically isolated (∼800 Ω inter-contact resistance) by etching the metal contact and the highly p doped GaAs from the upper surface of the semiconductor in a 4 μm wide channel between sections.

Assuming that above threshold gain pins at its threshold value, gth, then

$$g_{\text{th}}L = g(n_1)S_1 + g(n_2)S_2 \tag{1}$$

where $g(n)$ is the material gain as a function of carrier density n and S_1 and S_2 are cavity section lengths, defined by the segmented contact, that sum to the total cavity length, L. For a material with a sub-linear gain characteristic, such as that in Fig. 2, it is clear from (1) that a small reduction in the carrier density of section 1, n_1, demands a large increase in that of section 2, n_2, in order for the device to maintain laser action. Consequently, the average carrier density above threshold is not pinned and can be varied.

The carrier density dependence of the refractive index thus allows the optical path length of the laser cavity to also be varied above threshold and, as a result, the wavelengths of the cavity modes to be tuned over a range that is of the order of one mode spacing [10]. For a 1 mm long laser emitting at 720 nm, this equates to a modest tuning range of ∼0.1 nm.

2.2 Enhanced wavelength tuning

The wavelength tuning mechanism described in Section 2.1 assumes that gain is a function of carrier density alone. This is only true if the peak of the gain spectrum does not vary with carrier density. In reality, the spectral position of the gain peak is a product of the density of states distribution in the material and probability of those states being occupied. In most traditional materials such as bulk or quantum wells large changes in gain requirement can be satisfied with small changes in transition energy and the

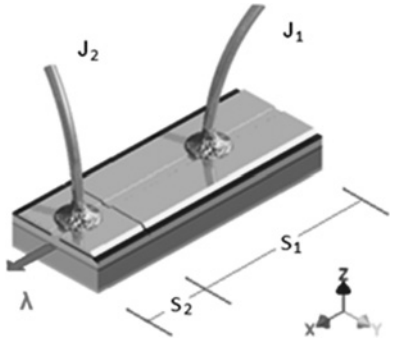

Fig. 1 *Oxide isolated stripe laser with the p-contact contact patterned into two segments with lengths S_1 and S_2 and operated at current densities J_1 and J_2, respectively*

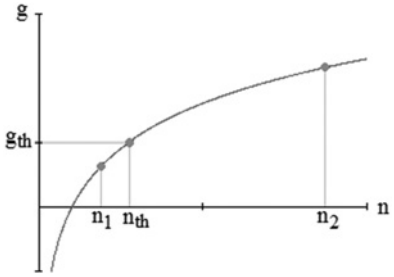

Fig. 2 *Gain against carrier density relation of a laser with a sub-linear gain characteristic showing how a reduction in the section 2 carrier density, n_2, produces an increase in section 2 carrier density, n_1*

assumption of wavelength independence is approximately correct with the tuning range dominated by the refractive index change. On the other hand, self-assembled quantum dot materials, with states distributed over a broad range of energies, can exhibit extremely large peak gain blue shifts with increasing current density. The net modal gain and absorption spectra of an InP quantum dot material, measured using the segmented contact method [13], are plotted in Fig. 3. The active region of this sample consists of five layers of self-assembled InP dots in 8 nm wide $Ga_{0.51}In_{0.49}P$ wells each separated by a 16 nm $(Al_{0.3}Ga_{0.7})_{0.51}In_{0.49}P$ barrier layer within a $(Al_{0.3}Ga_{0.7})InP/Al_{0.51}In_{0.49}P$ core/cladding waveguide.

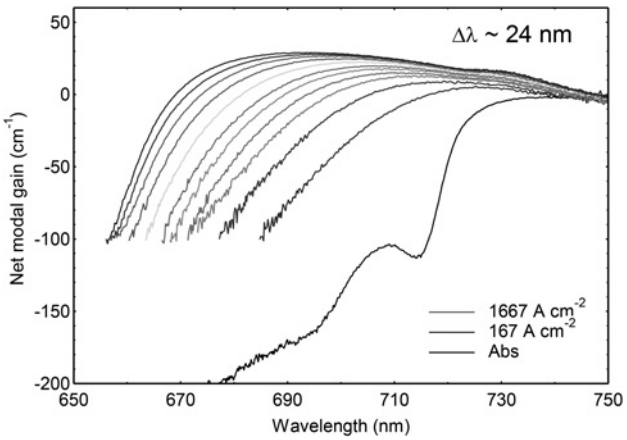

Fig. 3 *InP quantum dot net modal gain spectra measured as a function of injection current density exhibit a large peak gain blue shift with increasing injection*

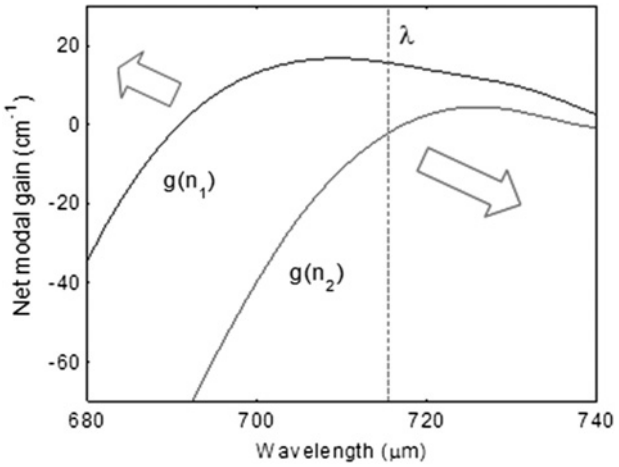

Fig. 4 *Gain spectra for the average carrier densities in sections 1and 2 (with a length ratio of 1:4) indicating how the lasing wavelength is determined by (2). A red shift by section 2 produces a corresponding blue shift in section 1 but asymmetry in the gradient of the gain spectra results in a net red shift of the laser*

The large peak gain spectral blue shift exhibited by this material system gives rise to an additional, potentially much enhanced, gain-levered tuning mechanism.

As with the refractive index tuning, and in accordance with (1), a reduction of the gain of one section must be compensated for by an increase in gain supplied by the other if laser action is to be maintained. However, in wavelength-dependent gain media, $g(n, \lambda)$, the lasing mode, which must correspond to the wavelength that experiences highest average round trip gain, does not simply follow the gain peak of either of the individual section, but rather falls at some point between them. Differentiating (1) w.r.t. wavelength yields the following condition

$$S_2 \cdot \frac{\mathrm{d}}{\mathrm{d}\lambda} g(n_2, \lambda) = -S_1 \cdot \frac{\mathrm{d}}{\mathrm{d}\lambda} g(n_1, \lambda) \tag{2}$$

In other words, the wavelength of the lasing mode in the gain-levered device can be approximated as the point where the gradients of the section-length weighted gain spectra of each individual section are equal and opposite, see Fig. 4.

Consequently, a reduction in section 2 carrier density brings about a corresponding reduction in the gain peak in that section but also shifts the peak to longer wavelength. The compensating increase in section 1 carrier density, required to maintain lasing, increases the gain but also shifts the gain peak to shorter wavelengths. Asymmetry in the gain spectrum produces a net wavelength shift towards longer wavelengths and therefore provides a means of tuning the lasing wavelength.

2.3 Enhanced wavelength tuning limits

The tuning range that can be accessed with this enhanced tuning mechanism ultimately depends on the shape of the material gain spectrum and how it varies with carrier density. Nevertheless, fundamental upper and lower wavelength limits can be defined in terms of device input parameters, namely the current densities applied to each section.

The short-wavelength limit occurs when the current densities in the two sections are equal that is $J_1 = J_2$. At this point the gain peaks of the two sections are aligned and so the lasing wavelength corresponds to mode that is closest to the peak. This point is therefore fixed by the threshold gain requirement of the laser and so is set by fixed device parameters such as the total cavity length and the reflectivity of the laser facets.

The long wavelength limit, as we define it here, occurs when only one of the sections is forward biased while the other is electrically unpumped. The un-pumped section then acts as a long-pass filter suppressing lasing at the peak of the other section. This long-wavelength limit is not quite as clearly defined as the short-wavelength limit as it will blue shift slightly above threshold with increasing output power as the un-pumped section is optically pumped by the pumped section. The long-wavelength limit could clearly be extended to longer wavelengths by applying reverse bias to the un-pumped section and red shifting the absorption edge via the Stark effect. However, this amounts to the introduction of an active loss element which constitutes a very different type of tuning mechanism to the one under discussion here.

Within these limits the lasing wavelength can theoretically be tuned continuously by simply varying the ratio of the input currents.

3 Results

To demonstrate the principle, in practice, the output spectra of a 1.9 mm long gain levered 50 μm wide oxide isolated stripe laser with InP dot active region and section length ratio 1:3.75 are plotted in Fig. 5 for the limiting cases described in Section 2.3. The tuning range of the device is taken as the difference between the peaks of the long- and short-wavelength limits, which in this case is $\Delta\lambda = (6.5 \pm 0.1)$ nm.

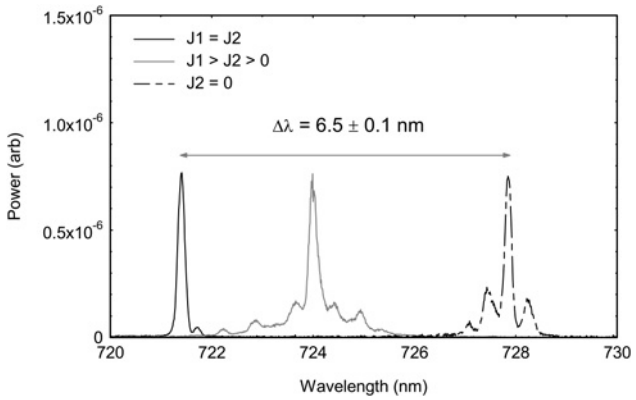

Fig. 5 *Lasing spectra of a 1.9 mm long device with a section length ratio of 1:3.75 showing the long- (dashed curve) and short (black curve)-wavelength limits with current densities (J_1 = 987 A/cm^2, J_2 = 0 A/cm^2) and ($J_1 = J_2$ = 326 A/ cm^2), respectively. Current densities of (J_1 = 747 A/cm^2, J_2 = 25 A/ cm^2) were used to produce the intermediate wavelength lasing spectrum (grey curve)*

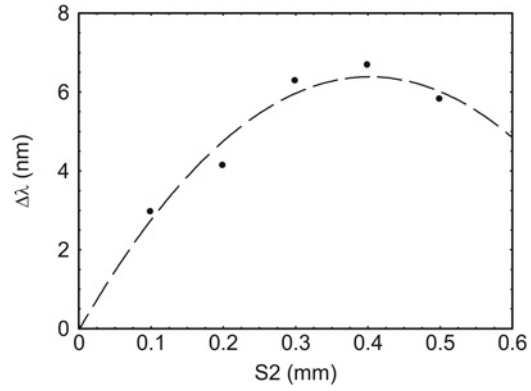

Fig. 6 *Tuning range of 1.9 mm long segmented contact lasers plotted as a function of increasing section 2 length. The saturation of the tuning range with larger section 2 lengths is caused by optical pumping. The polynomial data fit (dashed curve) has been included as a guide to the eye.*

Tested up to a front facet output power of 35 mW, the lasing wavelengths that set the long- and short-wavelength limits of the tuning range remain fixed. Above this value, lasing from side modes begins to affect the limits of the tuning range: for the short-wavelength limit, where the device is effectively operating as a single contact laser, this is a consequence of state filling in the quantum dot material. For the long-wavelength limit, modes appearing at wavelengths shorter than the limit are thought to result from the optical pumping mechanism described above.

In Fig. 6 the tuning range, as defined above, is plotted against varying section 2 length for a fixed overall device length of 1.9 mm.

Initially, the tuning range increases with increasing section 2 length, but, at a length of 0.4 mm ($S_2/S_1 = 0.21$), it reaches a peak and for $S_2 = 0.5$ reduces. The reduction of the tuning range at larger section 2 lengths is thought to result from section 2 blue shifting due to optical pumping. For a given material and a given device length, therefore, there exists an optimum section length ratio for the maximum tuning range.

4 Discussion

4.1 General device design rules

From these experimental observations we define a set of general design rules for the maximisation of the enhanced wavelength tuning range of a gain-levered device.

(i) The total cavity length should be as short as possible whilst maintaining the capacity for laser action when one section is un-biased. This maximises the blue shift of the short-wavelength tuning limit whilst allowing the full tuning range to be accessed.
(ii) Section 2 should be made as large as possible. This gives the largest red shift when un-pumped and therefore produces the largest overall tuning range.
(iii) The upper limit on the length of section 2 is theoretically when it equals that of section 1 that is $S_2 = S_1$. However, if section 2 is made longer than the optimum value, as is demonstrated in Fig. 6, the long-wavelength tuning limit starts to reduce due to the optical pumping effect. Ultimately the critical section 2 length is determined by the material gain parameters and therefore must be measured.

4.2 Material design

For a cleaved facet device, the lower limit on the total cavity length, set by design rule 1 in Section 4.1, is determined by the amount of optical gain that is available and the current density that can be supplied. The tuning range can therefore be increased by increasing the amount of gain provided by the material system. In the InP dot material the current density can be significantly reduced and to some extent the gain available can be increased by optimising the gallium fraction, x of the $Ga_xIn_{1-x}P$ material in the upper confining layer of the quantum dots [14]. The gain available can also be increased by increasing the dot density or by increasing the total number of DWELL layers in the active region. The latter effect increases the gain without affecting the dot state distribution and so has no detrimental effect on the long-wavelength limit. To increase the dot state distribution still further, there are a number of options that have previously been used to extend the emission range of superluminescent LEDs such as changing the composition [14] or the width [15] of the wells in the DWELL or optimising the post-growth rapid thermal annealing temperature [16].

5 Conclusions

Wavelength tuning in segmented contact lasers via the gain-lever effect results from two distinct mechanisms: refractive index tuning and material gain peak tuning. The degree to which each of

IET Optoelectron., 2016, Vol. 10, Iss. 2, pp. 66–69

these mechanisms contributes to wavelength tuning depends on the distribution of electronic states within the material itself. When the material gain peak tuning effect dominates we see a continuous wavelength tuning enhancement of around two orders of magnitude compared with that possible via the refractive index tuning effect that is one mode spacing. The total tuning range that can be achieved in a given material system can be maximised by optimising the device design parameters: total cavity length and the segmented contact length ratios.

6 Acknowledgments

This work was supported by EPSRC grant EP/L0050409/1. Information on how to access all data supporting the results in this article can be found at Cardiff University data catalogue at http://dx.doi.org/10.17035/d.2015.100115.

7 References

1 Grobe, K., Eiselt, M.l.H., Pachnicke, S., *et al.*: 'Access networks based on tunable lasers', *J. Lightwave Technol.*, 2014, **32**, (16), pp. 2815–2823
2 Zhang, J., Ansari, N.: 'Design of WDM PON with tunable lasers: the upstream scenario', *J. Lightwave Technol.*, 2010, **28**, (2), pp. 228–236
3 Choi, D., Yoshimura, R., Ohbayashi, K.: 'Tuning of successively scanned two monolithic Vernier-tuned lasers and selective data sampling in optical comb swept source optical coherence tomography', *Biomed. Opt. Express*, 2013, **4**, pp. 2962–2987
4 Phelan, R., Lynch, M., Donegan, J.F., *et al.*: 'Simultaneous multispecies gas sensing by use of a sampled grating distributed Bragg reflector and modulated grating Y laser diode', *Appl. Opt.*, 2005, **44**, (27), pp. 5824–5831
5 Numata, K., Chen, J.R., Wu, S.T.: 'Precision and fast wavelength tuning of a dynamically phase-locked widely-tunable laser', *Opt. Express*, 2012, **20**, (13), pp. 14234–14243
6 Telford, W.: 'Lasers in flow cytometry', *Methods Cell Biol.*, 2011, **102**, p. 375409
7 Zhang, D., Zhao, J., Yang, Q., *et al.*: 'Compact MEMS external cavity tunable laser with ultra-narrow linewidth for coherent detection', *Opt. Express*, 2012, **20**, (18), pp. 19670–19682
8 Ishii, H., Kasaya, K., Oohashi, H.: 'Narrow spectral linewidth operation (<160 kHz) in widely tunable distributed feedback laser array', *Electron. Lett.*, 2010, **4**, (10), pp. 714–715
9 Jayaraman, V., Mathur, A., Coldren, L.A., *et al.*: 'Extended tuning range in sampled grating DBR lasers', *IEEE Photonics Technol. Lett.*, 1993, **5**, (5), pp. 489–491
10 Lau, K.Y.: 'Broad wavelength tunability in gain-levered quantum well semiconductor lasers', *Appl. Phys. Lett.*, 1990, **57**, (25), pp. 2632–2634
11 Li, Y., Naderi, N.A., Kovanis, V., *et al.*: 'Enhancing the 3-dB bandwidth via the gain-lever effect in quantum-dot lasers', *IEEE Photonics J.*, 2010, **2**, (3), pp. 321–329
12 Vahala, K.J., Newkirk, M.A., Chen, T.R.: 'The optical gain lever: a novel mechanism in the direct modulation of quantum well semiconductor lasers', *Appl. Phys. Lett.*, 1989, **54**, (25), pp. 2506–2508
13 Blood, P., Lewis, G.M., Smowton, P.M., *et al.*: 'Characterisation of semiconductor laser gain media by the segmented contact method', *IEEE J. Quantum Electron.*, 2003, **9**, (5), pp. 1275–1282
14 Kasim, M., Elliott, S.N., Krysa, A.B., *et al.*: 'Reducing thermal carrier spreading in InP quantum dot lasers', *IEEE J. Sel. Top. Quantum Electron.*, 2015, **21**, (6), pp. 1–6
15 Ray, S.K., Groom, K.M., Liu, H.Y., *et al.*: 'Broad-band superluminescent light emitting diodes incorporating quantum dots in compositionally modulated quantum wells', *Jpn. J. Appl. Phys.*, 2006, **45**, pp. 2542–2545
16 Li, L.H., Rossetti, M., Fiore, A., *et al.*: 'Wide emission spectrum from superluminescent diodes with chirped quantum dot multilayers', *Electron. Lett.*, 2005, **41**, (1), pp. 41–43
17 Zhang, Z.Y., Hogg, R.A., Xu, B., *et al.*: 'Realization of extremely broadband quantum-dot superluminescent light-emitting diodes by rapid thermal-annealing process', *Opt. Lett.*, 2008, **33**, (11), pp. 1210–1212